Supporting Information

Porous Silica Nanospheres: A Nanoplatform Towards Protein Immobilization and Cogent Design of Biosensors for Aromatic Water Pollutant Detection.

Sumita Das,[a†] Subhankar Sahu,[a†] Rajdip Bandyopadhyaya,[b] and Ruchi Anand[a*]

[a]Department of Chemistry, Indian Institute of Technology Bombay, Powai, Mumbai 400076, India.

[b]Department of Chemical Engineering, Indian Institute of Technology Bombay, Powai, Mumbai 400076, India.

Email: ruchi@chem.iitb.ac.in

Supporting Experimental Methods

Synthesis of MCM-41 Silica Nanoparticles (MCM-41)

Mesoporous silica nanoparticles (MCM-41) were typically synthesized using the following protocol.[1] Initially, 0.25 g of CTAB (surfactant) was added in 120 mL of deionized water, followed by addition of 0.875 mL of 2 M NaOH to it. The resulting solution was stirred for 1 h at 300 rpm and 35 °C. Decane (0.6 mL, expander) was then added and the solution was further stirred for 4 h at 35 °C. Temperature was then raised to 80 °C and 1.25 mL of TEOS, (MCM-41 silica precursor) was added to the solution. Stirring was further continued for 30 min at 80 °C. After that the solution was cooled down to room temperature. The silica nanoparticles were then collected by centrifugation at 14000 rpm for 10 min. Solid products were filtered and washed several times using water. It was dried overnight in oven. Later, to remove the surfactant CTAB by calcination, the nanoparticles were heated in furnace at 540 °C for 6 h. The MCM-41 mesoporous silica was stored at room temperature prior to further use.

Synthesis of Non-porous Silica Nanoparticles (NPS)

Non-porous silica nanoparticles were synthesized using ethanol with ammonia solution as catalyst.[2] The reaction was carried out at 35◦C in a 250 ml flask with mechanical stirring at 300 rpm. Solution I containing KCl (0.0015 g), ethanol (38 ml), water (6 ml), and ammonia (3 ml) was added into the flask firstly, and then, solution II containing 58 ml of ethanol and 5.64 g of TEOS was added into the flask continuously by a syringe pump in 2 hours. After further reaction for 15 hours, the obtained microspheres were purified by centrifugation and washing with ethanol for three times. Finally, the microspheres were dried under vacuum at ambient temperature. The non-porous silica nanoparticles are designated as NPS.

MopR Biosensor Cloning and Protein Purification

Purified genomic DNA of *Acinetobacter calcoaceticus NCIB8250* is used for the amplification of the MopR gene of 1500 bp coding the A+C construct of 500 amino acid. This gene was then cloned into modified pET vector and transformed into *E. coli* BL21(DE3) pLysS cells. The transformed cells were plated onto Kanamycin and Chloramphenicol (concentrations 35µg/mL and 30µg/mL respectively) plate and incubated for 16h at 37^{o}C. The 5mL volume of LB media containing the above antibiotics in the same concentration as in the plate, were then inoculated with a colony from each of the plates to set up the pre-inoculum for large-scale growth. They were then grown overnight at 37 ^{o}C and 220 rpm in a shaker incubator. These 5 ml cultures were then inoculated in 5X1 litre of LB culture media (in presence of appropriate antibiotics in same concentrations as mentioned above). The large-scale culture media were then grown by shaking at 37 ^{o}C and 220 rpm, till the OD of the culture at 600 nm was ~0.4-0.7. Then they were induced by 0.8 mM IPTG (isopropyl-β-D-thiogalactopyranoside) and 5 mM $MgCl_2$ and growth was continued at a reduced temperature of 16 ^{o}C. After 16 hrs., the cells were harvested by centrifugation at 5000 rpm for 30 minutes.

MopR protein was purified using Ni-NTA resin by standard His-tagged affinity purification protocol. The composition of the buffers used in subsequent purification steps was as follows: lysis buffer (50mM Tris-HCl, pH 7.5; 5mM Imidazole; 350mM NaCl), wash buffer (50mM Tris-HCl buffer, pH 7.5; 20mM Imidazole; 250mM NaCl), and elution buffer (50mM Tris-HCl buffer, pH 7.5; 50-500mM Imidazole; 150mM NaCl). The eluted fractions were desalted using an EconoPac 10DG (Bio-Rad, CA, USA) column that was pre-equilibrated with a desalting buffer containing 25mM Tris-HCl buffer, pH 7.5; 100mM NaCl, 5% glycerol, and 0.5mM DTT. The desalted protein fractions were pooled and concentrated up to 10 mg/ml, as determined by the Bradford assay using Bovine

Serum Albumin (BSA) as a standard. The protein fractions were then flash-frozen in liquid N_2 and stored at −80 °C until they were used. The purity of the protein was verified by running a 10% SDS-PAGE followed (Fig. S4) by Coomassie Blue (HiMedia, Mumbai, India) staining.

Instrumentation

Transmission electron microscopy (TEM) analysis of the bare and functionalized porous silica nanospheres was done on JEOL (Model- JEM 2100F) at 200 kV. Dynamic light scattering (DLS) measurements were performed on Anton Parr Litesizer 500. Nitrogen sorption measurements were conducted by using a Quantachrome Autosorb AS-1 at liquid nitrogen temperature (77 K). The Brunauer−Emmett−Teller (BET) method was used to calculate the average pore diameter, pore volume and surface area. Circular dichroism (CD) spectra of MopR and MopR with pSN-1 silica nanospheres were recorded on JASCO, J-815 CD spectrometer. Fourier transform infrared (FT-IR) spectra were recorded on Perkin Elmer (Spectrum One). All the optical response from the malachite green dye-based ATPase assay were monitored at 630 nm through IMPLEN NanoPhotometer (NP80).

Table S1. Physical properties of bare synthesized porous silica nanospheres at different synthesis conditions.

Sample	Reaction time (h)	Reaction temperature (° C)	TEOS in Cyclohexane (v/v%)	Average Particle size (nm) (From TEM)	Average Particle size (nm) (From DLS)	Specific Surface area (m^2/g)	Pore volume (cc/g)	Average pore diameter (nm)
pSN-1	5	80	40	52.3±8	68	496.1	1.12	9.04
pSN-2	10	80	40	47.3±8	54	260.3	0.72	11.05
pSN-3	15	80	40	44.2±6	58	182.1	0.64	14.01
pSN-4	10	80	10	37.5±7	44	308.7	0.55	7.12
pSN-5	10	60	40	43.2±7	55	138.0	0.44	12.78

Table S2. Comparison of this research with other commonly reported enzyme-based phenol biosensors.

	Enzyme Used	Details	Analyte, LOD	Selectivity	Reference
1.	Tyrosinase	Au nanoparticles (AuNPs) are electrodeposited onto a disposable screen-printed carbon electrode and tyrosinase is then covalently immobilized on the AuNP's. Electrochemical biosensor.	Phenol, 0.5 µM	++	3
2.	Tyrosinase	Tyrosinase immobilized on 2D pnictogen-based nano-sheet. Electrochemical biosensor.	Phenol, 0.5 µM	+++	4
3.	Tyrosinase	Tyrosinase immobilized chitosan film. Optical biosensor.	Phenol, 1 µM	+	5
4.	Tyrosinase	A long-period fiber grating coated with a tyrosinase-entrapped polyacrylamide gel is used. Optical biosensor.	81 µM	+	6
5.	Tyrosinase	Gold nanoparticles screen-printed electrodes were thoroughly modified with tyrosinase (Tyr-AuNPS-SPCEs), which was immobilised on the surface by crosslinking with glutaraldehyde is used.	1.2 µM	+	7
6.	Laccase	Molecular absorption and fluorescence properties of laccase is used. Optical biosensor.	Phenol, 9 µM	++	8
7.	MopR	MopR coated porous silica nanospheres is used. Colorimetric biosensor.	Phenol, 0.1 µM	+++	This Work

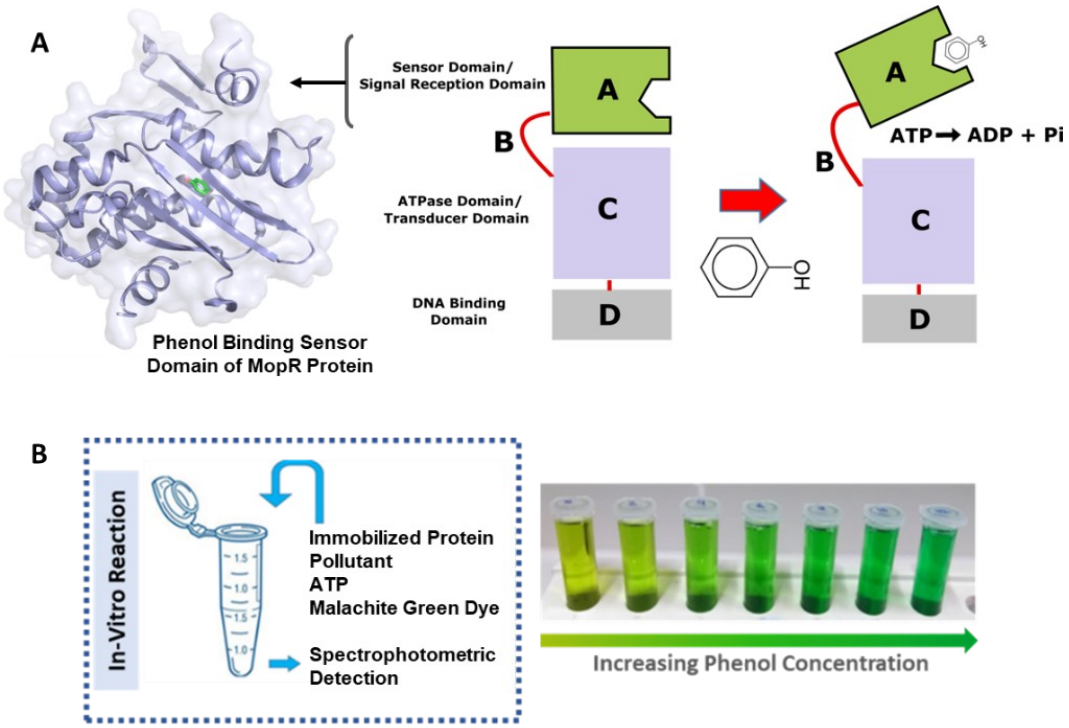

Fig. S1 (A) Domain architecture and biochemistry of MopR protein. The protein has three major domains – A: sensor domain responsible for phenol binding; C: ATP hydrolysis domain; D: DNA binding domain. Cartoon representation of the structure of MopR A domain bound to phenol is shown at left hand side (PDB ID 5KBE). The phenol is depicted with carbon atoms as green colour stick and oxygen atom as red representation. The B linker connects the A and C domain.[9] The phenol unbound form of the protein (left) is considered the inactive form while the phenol bound form results in activation of the protein via a conformational rearrangement that triggers ATP hydrolysis activity. The induced hydrolysis activity is proportional to the amount of phenol bound to the sensor domain which is quantitated by the inorganic phosphate generated from the reaction via a malachite dye-based complexation.[10] (B) The in-vitro reaction setup is shown. The pSN strips are treated with water samples and required chemical components as shown and subjected for malachite green assay, the final green colour profile varies depending on the phosphate formed which is proportional to the phenol concentration.

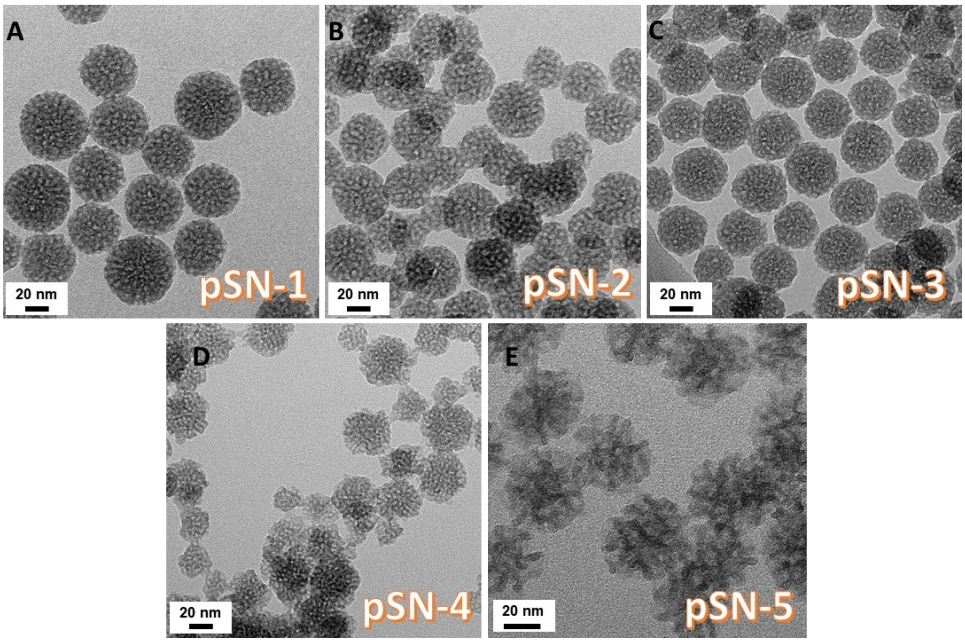

Fig. S2 High magnification TEM images of porous silica nanospheres of (A) pSN-1, (B) pSN-2 (C) pSN-3 (D) pSN-4, and (E) pSN-5 respectively. Homogeneous distribution and porous nature of the particles are clearly visible in the images.

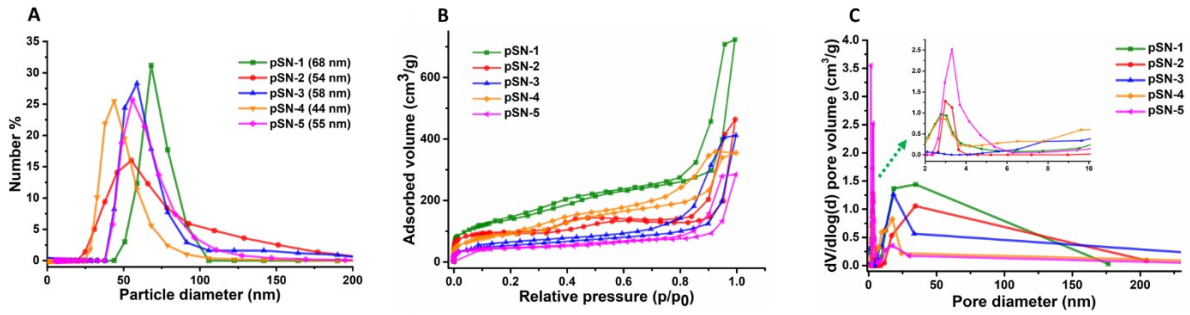

Fig. S3 (A) Particle size distribution from dynamic light scattering (DLS). (B) Nitrogen adsorption/desorption isotherm curves exhibiting type-VI mesoporous hysteresis loop. (C) BJH pore size distribution of all synthesized porous silica nanospheres.

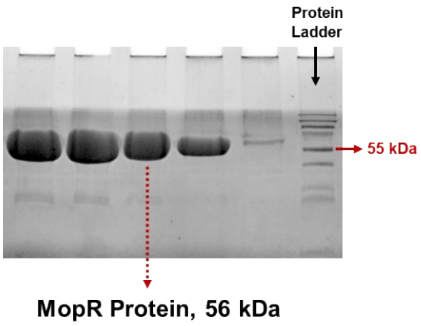

Fig. S4 SDS-PAGE gel showing pure MopR native protein of 500 amino acid residues (MopR^{AC}, Molecular Weight ~56 kDa).

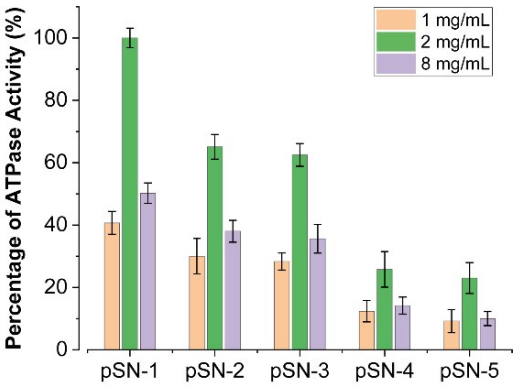

Fig. S5 Phenol sensing activity of the porous silica nanospheres at different concentrations. pSN-1 exhibits highest response at all tested concentration.

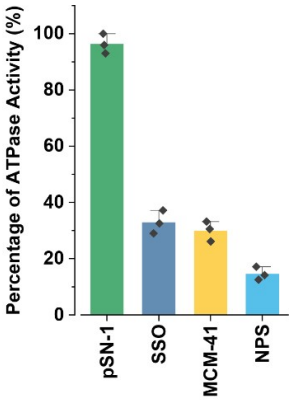

Fig. S6 Comparison of activity of MopR phenol biosensor when immobilized on different types of silica nanoparticles. The pSN-1 is most satiable for protein immobilization sustaining the activity of the protein. Commercially available silica - SSO, synthesized MCM-41 - MCM-41 and non-porous silica - NPS.

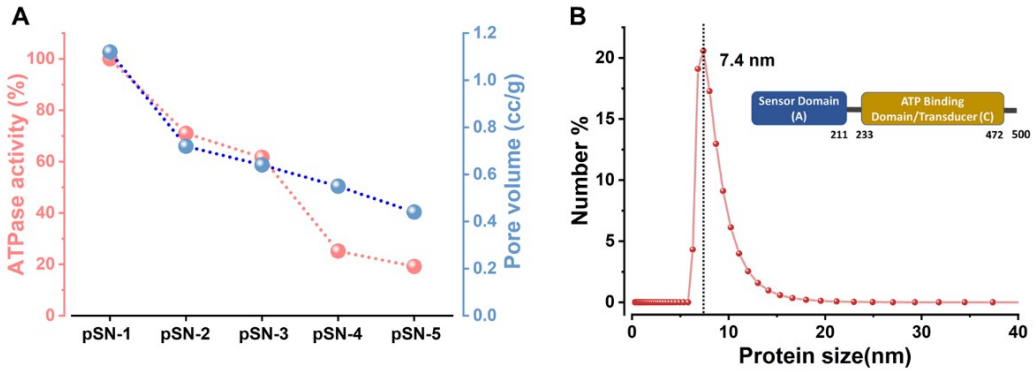

Fig. S7 (A) Comparison of total pore volume of pSNs with their ATPase activitites (i.e. phenol sensing signal). (B) DLS measurement of the MopR^{AC} protein used for immobilization fabrication of pSN strips.

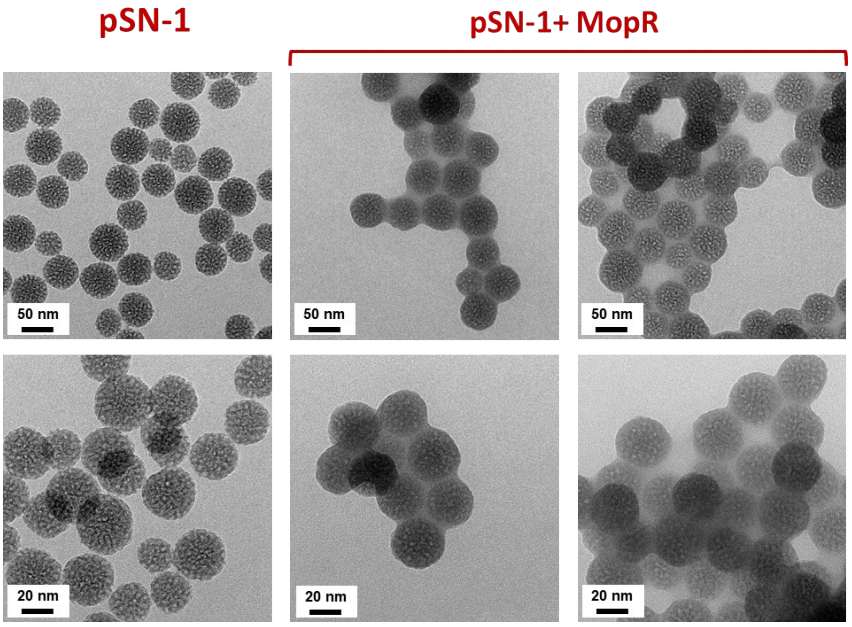

Fig. S8 Bright field images of bare pSN-1 silica nanospheres and with MopR protein in different magnifications.

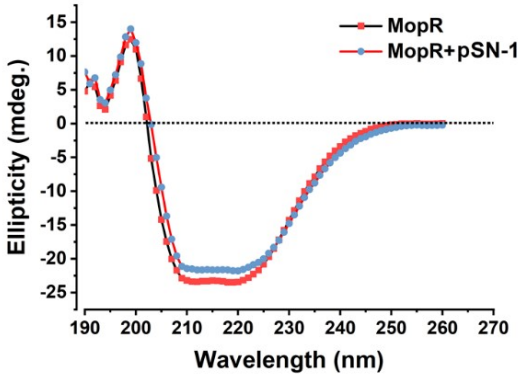

Fig. S9 Circular dichroism (CD) spectra of protein MopR in presence and absence of pSN-1. Very minimal loss of protein conformation can be seen for MopR in presence of pSN-1.

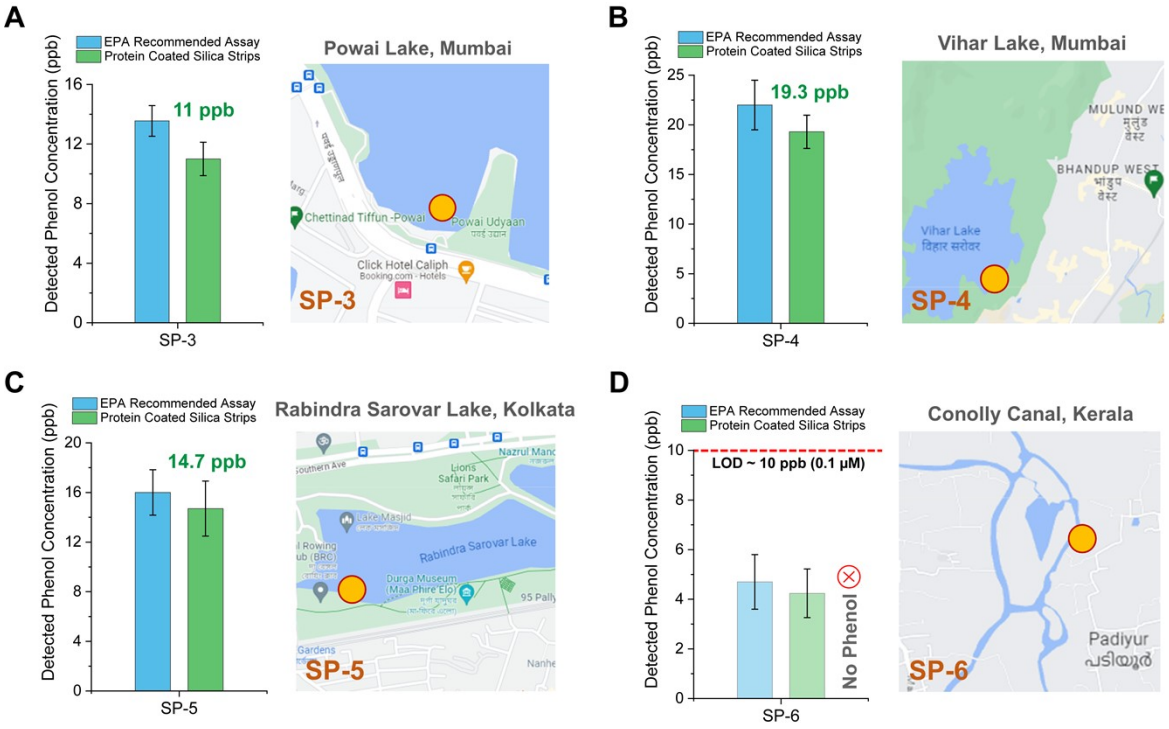

Fig. S10 Analysis of phenol content in water samples collected from different parts of India – (A) Powai Lake, Mumbai (B) Vihar Lake, Mumbai (C) Rabindra Sarovar Lake, Kolkata and (D) Conolly Canal, Kerala. The pSN-1 biosensing strips have similar phenol detection efficiency as compared to the standard EPA assay. The detected phenol concentration through the MopR-pSN-1 strips is given above each bar. The map location is shown for each sample.

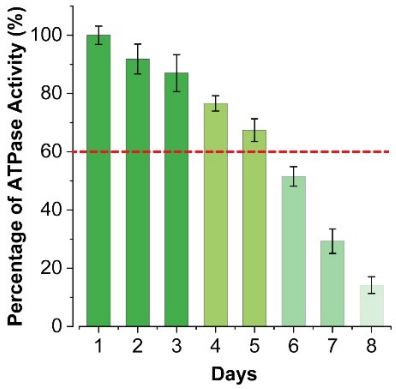

Fig. S11 Shelf-life of the MopR-pSN-1 strips. The strips are stable for 5 days with phenol detection response >60% (red dashed line).

References:

1 K. Saini and R. Bandyopadhyaya, Transferrin-Conjugated Polymer-Coated Mesoporous Silica Nanoparticles Loaded with Gemcitabine for Killing Pancreatic Cancer Cells, *ACS Appl. Nano Mater.*, 2020, **3**, 229–240.

2 X. Lei, B. Yu, H. L. Cong, C. Tian, Y. Z. Wang, Q. Bin Wang and C. K. Liu, Synthesis of monodisperse silica microspheres by a modified stöber method, *Integr. Ferroelectr.*, 2014, **154**, 142–146.

3 M. Nurul Karim and H. J. Lee, Amperometric phenol biosensor based on covalent immobilization of tyrosinase on Au nanoparticle modified screen printed carbon electrodes, *Talanta*, 2013, **116**, 991–996.

4 C. C. Mayorga-Martinez, R. Gusmão, Z. Sofer and M. Pumera, Pnictogen-Based Enzymatic Phenol

Biosensors: Phosphorene, Arsenene, Antimonene, and Bismuthene, *Angew. Chemie Int. Ed.*, 2019, **58**, 134–138.

5 J. Abdullah, M. Ahmad, N. Karuppiah, L. Y. Heng and H. Sidek, Immobilization of tyrosinase in chitosan film for an optical detection of phenol, *Sensors Actuators B Chem.*, 2006, **114**, 604–609.

6 S. K. Mishra and K. S. Chiang, Phenolic-compounds sensor based on immobilization of tyrosinase in polyacrylamide gel on long-period fiber grating, *Opt. Laser Technol.*, 2020, **131**, 106464.

7 M. Cerrato-Alvarez, E. Bernalte, M. J. Bernalte-García and E. Pinilla-Gil, Fast and direct amperometric analysis of polyphenols in beers using tyrosinase-modified screen-printed gold nanoparticles biosensors, *Talanta*, 2019, **193**, 93–99.

8 J. Sanz, S. de Marcos and J. Galbán, Autoindicating optical properties of laccase as the base of an optical biosensor film for phenol determination, *Anal. Bioanal. Chem.*, 2012, **404**, 351–359.

9 S. Ray, M. J. Gunzburg, M. Wilce, S. Panjikar and R. Anand, Structural Basis of Selective Aromatic Pollutant Sensing by the Effector Binding Domain of MopR, an NtrC Family Transcriptional Regulator, *ACS Chem. Biol.*, 2016, **11**, 2357–2365.

10 S. Ray, S. Panjikar and R. Anand, Structure Guided Design of Protein Biosensors for Phenolic Pollutants, *ACS Sensors*, 2017, **2**, 411–418.